

# Nondestructive Inspection of the Diameter of Reinforcing Bars in Concrete Using an Electromagnetic Wave (Radar)

Halima BEGUM\*, Masayuki OKAMOTO\* and Shogo TANAKA\*

For the measurement of the diameter of a deformed bar in concrete, an electromagnetic wave (EMW) radar is used which scans along the bar. In our previous method, the radar was run while keeping it in contact with the concrete surface, because this is the usual procedure of scanning with a radar. This resulted in a larger angle of incidence of the EMW to the bar, which consequently elevated the frequency of receiving reflections both from the rib and the base of the bar simultaneously. Therefore, the frequency of erroneous measurement of the propagation time of the EMW to the point on the bar just below the radar and back became large. This consequently affected the success in the measurement of the diameter greatly. Therefore, the present paper proposes a new method. The new method introduces a better scanning procedure, which involves the lift-off of the radar during the scanning. Experiments show the comparison of the successful measurements with and without the lift-off of the radar and verify the effectiveness of the method.

**Key Words:** non-destructive inspection, diameter, reinforcing bar, electromagnetic wave (radar), lift off, Kalman filter, maximum likelihood method.

## 1. Introduction

Reinforcing bars are used in concrete structures to endure any tensile force<sup>1)</sup>. Specially, deformed bars are used for their better adherence to the concrete. A deformed bar has some protruding parts from its base, known as the ribs, which are responsible for the bonding strength with the concrete. The spacing between the ribs, i.e. the rib's pitch, is related to the diameter of the deformed bar<sup>2)</sup>.

The selection of the deformed reinforcing bars of adequate diameter must of course be made to avoid a risk of collapse of concrete structures. But, sometimes to minimize the cost of construction, bars of smaller diameters than the recommended ones are used. To check whether the guidelines about the diameter of the bar are followed properly, inspection is generally conducted. But, the inspection is done after the construction, regrettably. That's why we have a great demand for a reliable method to measure the diameter of the bar nondestructively.

The authors previously proposed a method for the non-destructive inspection of the diameter of the bar using an electromagnetic wave (EMW) radar<sup>2)</sup>. The method focused on the rib's pitch measurement and then indirectly measured the diameter from the relationship between the rib's pitch and the diameter of the bar. To measure the

rib's pitch by the method, the bar was scanned along its length with a radar. During the scanning, the radar was in contact with the concrete surface, because this manner of scanning is usually practiced. From the received signal at each scanning point, the information on the propagation time of the EMW to the bar and back was measured by a pattern matching procedure described in the previous method<sup>2)</sup>. But in our previous method, the EMW transmitted into the concrete had a large angle of incidence to the bar. So the frequency of simultaneously obtaining reflections both from the rib and the base became higher. Therefore, the measurement of the propagation time of the EMW reflected from the point on the bar just below the scanning point was difficult.

That's why we propose here to lift the radar off the concrete surface during the scanning of the bar. By increasing the lift-off we can expect to obtain a smaller angle of incidence of the EMW to the bar. That is, we can expect to realize an almost vertical propagation path of the EMW inside the concrete. This will consequently enable us to obtain a much more accurate propagation time of the reflected EMW from the point (on the bar) just below the scanning point.

Then, by applying our previous signal processing method<sup>2)</sup> (i.e., the method using a Kalman filter and maximum likelihood) to the propagation time variation along the length of the bar, we can achieve a much more accurate measurement of the rib's pitch, i.e., that of the diameter of the bar. Experiments will show the reliability

---

\* Graduate School of Science and Engineering,  
Yamaguchi University.  
2-16-1, Tokiwadai, Ube, 755-8611, Japan  
(Received December 26, 2008)

and effectiveness of our new method.

## 2. Overview of the previous method

In our previous method<sup>2)</sup> a radar scanned the bar along its length while being in contact with the concrete surface. At each scanning point, the received signal  $r(t)$  is modeled as the linear combination of the surface wave (the reflected wave from the surface) and the reflected EMW from the bar as below<sup>2) 3) 4)</sup>

$$\tilde{r}(t) = p_1 r_s(t - T_1) + p_2 r_o(t - T_2) \quad (1)$$

where  $r_s(t)$  and  $r_o(t)$  are respectively the fundamental surface wave and the fundamental reflected EMW signal from the bar. Here,  $T_1$  and  $T_2$  are the propagation times of the surface wave and the EMW reflected from the bar respectively. Again  $p_1$  and  $p_2$  denote the linear combination coefficients of the surface wave and the reflected EMW.  $r_s(t)$  and  $r_o(t)$  are known a priori from experiments. The unknown parameters in the modeled received signal are  $p_1$ ,  $p_2$ ,  $T_1$  and  $T_2$ .

To obtain the propagation times of the EMWs, pattern matching<sup>2) 3) 4)</sup> is performed between the actual and the modeled received signal. The values of  $p_1$  and  $p_2$  being obtained analytically for any  $T_1$  and  $T_2$  (see appendix),  $T_1$  and  $T_2$  are the only parameters to be solved numerically.

The evaluation function  $\theta$  for the pattern matching is expressed as

$$\theta = \cos^{-1} \left( \frac{(r(t), \tilde{r}(t))}{\|r(t)\| \|\tilde{r}(t)\|} \right) \quad (2)$$

where,  $(\cdot, \cdot)$  and  $\|\cdot\|$  represent the inner product and the norm in Hilbert space respectively. From the values of  $T_1^*$  and  $T_2^*$  for which  $\theta$  is minimized, we can obtain the optimal propagation time (i.e.,  $T_2^*$ ) of the EMW reflected from the bar just below the scanning point<sup>2)</sup>.

Now, the propagation time variation of the EMW reflected from the bar along the length of the bar is periodic in nature<sup>2)</sup> and thus is modeled as a linear combination of several sinusoidal functions with an additional bias. That is,

$$y(l) = z_0 + \sum_{i=1}^n z_i(l) \quad (3)$$

where  $l$  represents the scanning distance and  $z_0$  is the bias and

$$z_i(l) = a_i \sin(\omega_i l + \phi_i) \quad (4)$$

with  $\omega_i = (2\pi/L)i$ . Here,  $L$  corresponds to the rib to rib distance i.e. the rib's pitch, while  $i = 1$  corresponds to the fundamental frequency component of the sinusoidal wave and  $i = 2, 3 \dots n$  correspond to the harmonic frequency

components. Also,  $\phi_i$  denotes the phase angle.

Now, by defining the state vector  $\mathbf{x}(l)$  as  $\mathbf{x}(l) = (z_0, z_1, \dot{z}_1, z_2, \dot{z}_2, \dots, z_n, \dot{z}_n)^T$ , variation of the propagation time is modeled as an output of a dynamic system<sup>2) 5)</sup>. The estimation of  $\mathbf{x}(l)$  is performed using a Kalman filter for different assigned values of  $L$ .

The optimal value of  $L$  (i.e.  $L^*$ ) is obtained by maximizing the likelihood function

$$\prod_{k=1}^K p(y_k/L, Y^{k-1}) \quad (5)$$

with respect to  $L$ . In Eq.(5),  $p(y_k/L, Y^{k-1})$  is a conditional probability density function for  $y_k$  for a given observation sequence  $Y^{k-1} = \{y_1, y_2, \dots, y_k\}$  and the assigned parameter  $L$ . Once the rib's pitch is solved, the diameter of the deformed bar can easily be obtained from the standard table relating the rib's pitch and the diameter of the bar.

## 3. Proposed scanning procedure

During the scanning with the radar along the bar, the radar transmits an EMW signal at each scanning point. Due to the difference in permittivity between the air and the concrete, a part of the EMW reflects from the concrete surface<sup>6)</sup>. The other part of the EMW transmits into the concrete and reflects from the bar to go back to the receiver.

In the previous method, the radar scanned the bar while being in contact with the concrete surface, i.e. the scanning was performed with no lift-off. In the situation the propagation path of the EMW from the radar to the bar and vice versa are far from that under the Snell's law. This is because the wave length of the EMW is much larger than the gap between the radar base and the concrete surface. Note that both the transmitter and the receiver are attached on the base of the radar. At that case the emitted EMW is expected to fall on the concrete surface almost vertically (see Fig.1(a)). Therefore, the angle of incidence  $\theta_1$  of the EMW becomes large as shown in Fig.1(a). As a result, frequency of simultaneous reception of the reflected waves both from the rib and the base, instead of obtaining reflection from only the point on the bar just below the scanning point, is high and thus it becomes difficult to obtain the propagation time of the EMW reflected from the bar just below the scanning point. This is caused from the non-sharpness of the directivity characteristics of the radar.

To avoid this, we propose here to lift-off the radar during the scan. With the increase of the lift-off the propa-

gation path is expected to tend to follow the Snell's law. As a result, the angle of incidence  $\theta_2$  becomes smaller as in Fig.1(b). Such smaller incidence and reflection angles mean an almost vertical propagation of the EMW to and from the bar inside the concrete. This minimizes the frequency of simultaneous reception of any unwanted reflected waves. So, at that case we can expect to get a received signal as composed of the reflected waves from the surface and the bar just below the scanning point only. And by such a scanning, we get much more informative propagation time variation which enables us to guess the accurate shape of the bar, i.e., the shape of periodical change of the base and the rib.

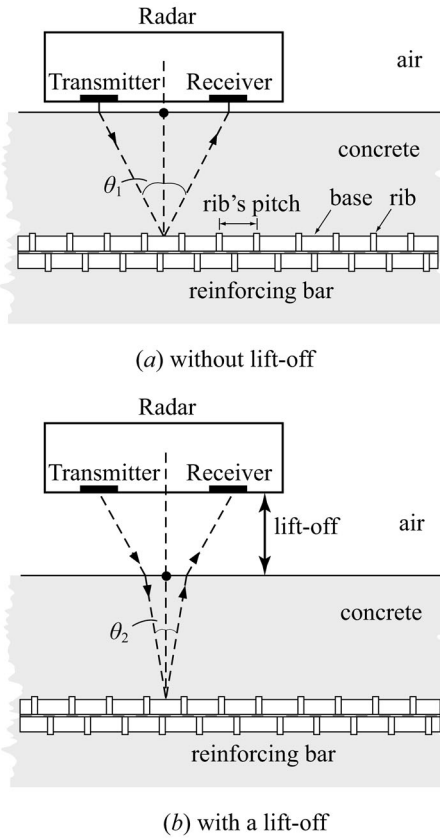


Fig. 1: Effect of the lift-off on the incidence angle of the electromagnetic wave

#### 4. Experimental results

The EMW radar used in the experiment was manufactured by Japan Radio Co. Ltd. The radar (bow-tie type) has separate transmitter and receiver antennae on the base of the radar with the center to center distance of 69mm between them. The specifications of the radar are: central frequency 800 MHz and sampling period  $\Delta T = 0.04$  ns. The radar sends and receives EMW

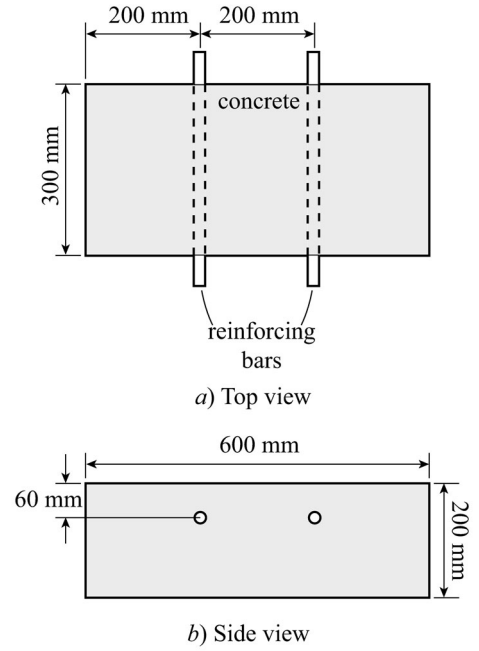


Fig. 2: Test specimen

signal at 5mm pitch.

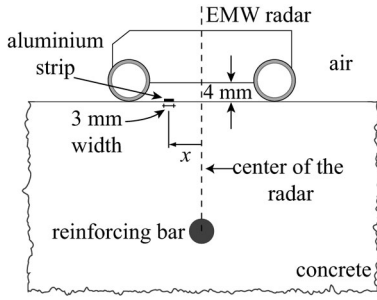
The reinforced concrete specimen we used has D19 type bars placed at 60mm depth from the concrete surface as shown in Fig.2. According to JIS standards<sup>2)</sup>, the diameter of this type of deformed bar is 19.1mm, while the rib's pitch can take a value between 11.1mm and 13.4mm. However, the average rib's pitch of the bar in the test specimen is 12.08mm with a standard deviation of 0.4mm.

Experiments were conducted in two steps. The first experiment is to observe the effect of the lift-off of the radar on the propagation path of the EMW from the radar to the bar and vice versa. The second experiment is to verify the effectiveness of the new approach in measuring the diameter non-destructively.

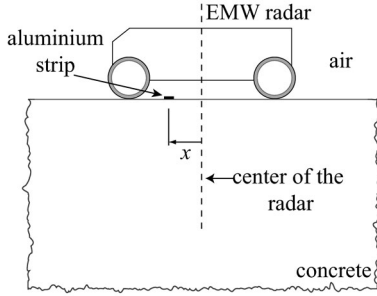
##### 4.1 The effect of the lift-off on the propagation path of the EMW signal from the radar to the bar and vice versa

The radar is first placed over the concrete surface just over a reinforcing bar with the radar axis perpendicular to the bar. This is to identify the propagation path of the radar when it has no lift-off. By the way, strictly speaking, the substantial air gap between the radar base (or the surface of the transmitter and the receiver) and the concrete surface for the formal 0mm lift-off is 4mm.

Next, a thin strip of aluminium having a dimension of 200mm×3mm is placed on the concrete surface underneath the radar at a distance  $x$  from the radar center (see Fig.3(a)). Here,  $x$  is taken positive for the positions to



a) position of the aluminium strip in the presence of the bar



b) position of the aluminium strip in the absence of bar

Fig. 3: Experimental set up for identifying the propagation path of the EMW to the bar and back to the radar

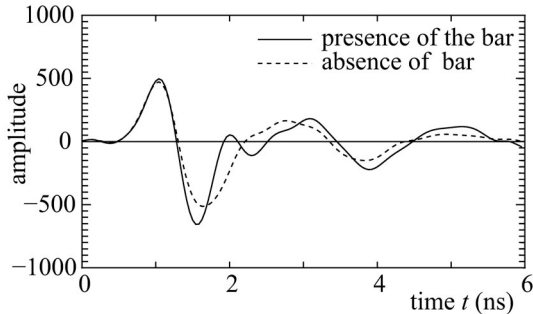


Fig. 4: Received signals in the presence and absence of the bar with the position of the aluminium strip at  $x = -20\text{mm}$

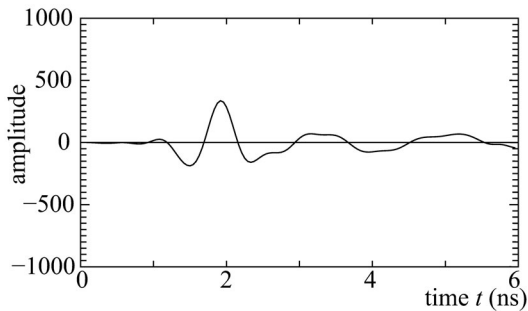


Fig. 5: Difference signal of the two received signals in Fig. 4

the right side of the radar center and negative for the positions to the left side. For this experimental set up, the radar receives three reflected EMWs from the concrete surface, the aluminium strip and the bar.

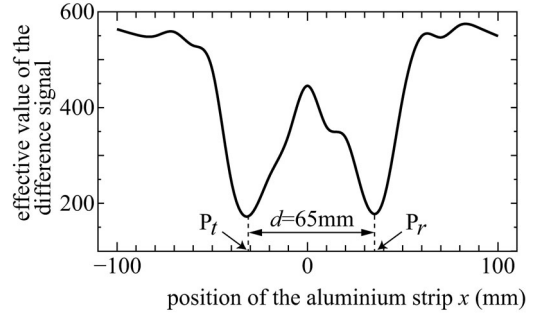


Fig. 6: Effective value of the difference signal versus the position of the aluminium strip for the case of lift-off 0mm

Now, keeping the aluminium strip at the same distance  $x$  from the center of the radar, we obtain a received signal by the radar for the case of no bar in the concrete (see Fig. 3(b)). For this set up, the received signal contains only reflected EMWs from the concrete surface and the aluminium strip. For reference, Fig. 4 shows the two received signals in the presence and absence of the bar when  $x = -20\text{mm}$ .

Now the difference between the two received signals shown in Fig. 5 is the reflected wave signal from the bar only for the aluminium strip at  $x = -20\text{mm}$ . The effective value of the difference signal represents the strength of the reflected wave from the bar. For different positions of the strip, the effective values of the difference signals are calculated and plotted in Fig. 6. Here,  $P_t$  and  $P_r$  represent the positions of the strip at which the effective values of the difference signals are minimum.

By placing the strip at  $P_t$ , we block the EMW from the radar to the concrete. Similarly, by placing the strip at  $P_r$ , we prevent the reflected EMW from the bar from going back to the receiver. In both cases the radar does hardly receive reflected EMWs from the bar.

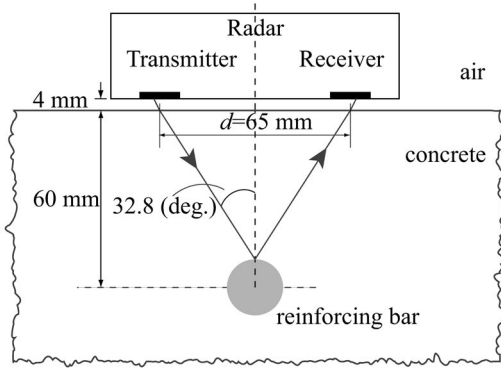
The distance  $d$  between the positions  $P_t$  and  $P_r$  for the formal 0mm lift-off is found to be 65mm which is very close to the specified value 69mm of the distance between the transmitter and receiver of the radar.

Now, by changing the formal lift-off of the radar from zero to 10 and 20mm respectively, the change in  $d$  is calculated. Table 1 lists the distance  $d$  between  $P_t$  and  $P_r$  obtained for each of the lift-offs. From the table we can see that as the lift-off increases, the value of  $d$  decreases.

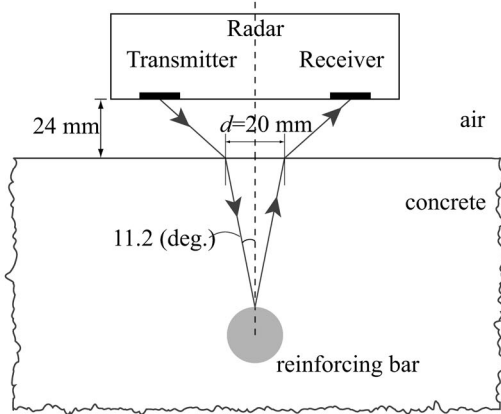
Fig. 7 shows the propagation paths from the radar to the bar and back for the two cases of the formal lift-offs 0mm and 20mm using the values of their corresponding  $d$  in Table 1. We can see that the angle of incidence and reflection on the bar for the case of formal lift-off 20mm is much smaller than that for the formal lift-off 0mm. For

Table 1: Distance between the two minima of the effective value of the difference signal

| formal lift-off (mm) | substantial lift-off (mm) | distance $d$ (mm) |
|----------------------|---------------------------|-------------------|
| 0                    | 4                         | 65                |
| 10                   | 14                        | 50                |
| 20                   | 24                        | 20                |



a) the propagation path for the formal lift-off 0mm



b) the propagation path for the formal lift-off 20 mm

Fig. 7: Comparison of the propagation paths of the EMWs from the radar to the bar for the formal lift-offs 0mm and 20mm

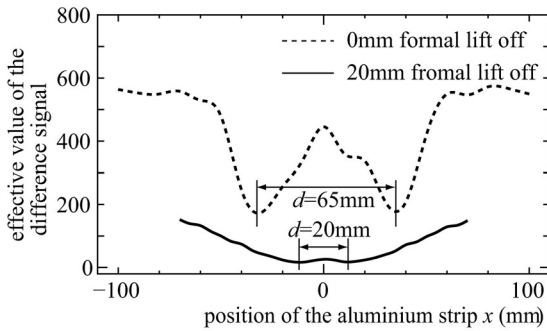


Fig. 8: Comparison of the effective values of the difference signals for the formal lift offs 0mm and 20mm

the 20mm formal lift-off, the angle of incidence to the bar obtained from the experiment is 11.2 deg, which is very close to the angle of incidence 13.23 deg calculated according to the Snell's law. So, we can say that with the increase of the lift-off the propagation path tends to follow the Snell's law and almost vertical incidence and reflection of the EMW to and from the bar is realized.

In **Fig.8** we compare the effective values of the reflected wave from the bar for the formal lift-offs 0mm and 20mm. We observe that the effective values of the difference signals for the lift-off 20mm are by far smaller than those obtained for the lift-off 0mm. So, we can say that, although with the increase of the lift-off almost vertical incidence and reflection to and from the bar is realized, the strength of the reflected wave from the bar decreases. Thus, we can conclude that further increase of the lift-off to obtain vertical incidence and reflection of the EMW to and from the bar may not yield any fruitful result, because at that case the EMW emitted from the radar merely injects into the concrete and consequently the reflected EMW from the bar is hardly received by the radar. Therefore, we consider the formal lift-off 20mm may be the limit. The conclusion is proved later in the next section.

#### 4.2 Measurement of the diameter of the bar

To obtain the propagation time variation of the EMWs reflected from the bar, the radar is run along the length of the bar, while being lifted off the concrete surface. We scanned the bar with the formal lift-off set as 0, 5, 10, 15, 20 and 25mm respectively and for each of the cases the propagation time variation is obtained<sup>2)</sup>. **Fig.9** shows the variation in the propagation time along the length of the bar while the formal lift off is 20mm.

We can see a low frequency bias in the variation. This might have resulted from the fact that the scanning line of the radar is not exactly parallel to the bar. To obtain the relative variation of the propagation time, we remove the low frequency component from the variation.

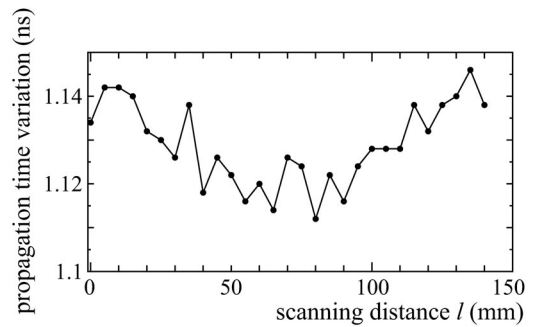


Fig. 9: Propagation time variation for the radar formally lifted 20mm off the concrete surface

For this purpose, we used a 7-point moving average filter. Since the allowable ranges of ribs' pitches of all the bars must lie within the passband of the filter, so considering the frequency characteristics of the filter, a 7 or a higher point moving average filter is desirable. But the number of data points in the filtered output reduces with the use of higher point moving average filter. That's why we consider to use the 7-point moving average filter here. **Fig.10** shows the relative variation in the propagation time after removing the low frequency component, which is treated as a new observation sequence in applying our previous signal processing method<sup>2)</sup>.

For each lift-off, we scan with the radar for 15 times and obtained the corresponding new observation sequences. We then analyze the observation sequences with our previous method<sup>2)</sup> i.e. the method using Kalman filter and maximum likelihood method.

The success rate in measuring the diameter of the bar for the different lift-offs is listed in **Table 2**. From the table we can see that with the increase of the formal lift-off up to 20mm the success rate increases monotonically. The reason is that with the increase of the lift-off the frequency of simultaneous reception of the reflected waves from the base and the rib of a bar decreases and thus the frequency of obtaining the informative propagation time

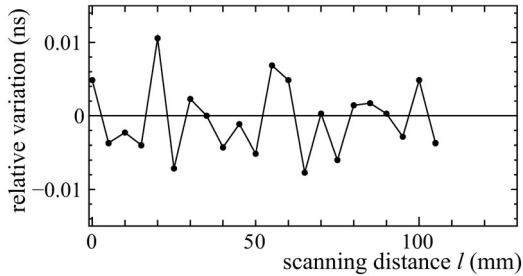


Fig. 10: Observation sequence after removing the low frequency component from the propagation time variation in Fig.9

Table 2: Measurement results for different lift-offs of the radar

| formal lift-off (mm) | trials succeeded (%) | normalized difference between the two largest extrema in likelihood, $Q$ (%) |       |       |
|----------------------|----------------------|--|-------|-------|
|                      |                      | minimum  | mean  | std   |
| 0                    | 80                   | 0.26   | 4.72  | 6.79  |
| 5                    | 80                   | 0.73   | 5.98  | 5.21  |
| 10                   | 93                   | 1.03   | 6.04  | 3.8   |
| 15                   | 100                  | 1.4  | 6.99  | 3.83  |
| 20                   | 100                  | 2.4  | 12.14 | 10.13 |
| 25                   | 87                   | 1.4  | 7.4   | 5.5   |

std: standard deviation

variation along the length of the bar increases.

However, we can see that with the increase of the lift-off the strength of EMW injection into the concrete as well as that of the EMW signal reflected from the bar decreases, making it difficult to obtain an adequate information on the propagation time of the EMW. As a result, success in the measurement of the diameter starts decreasing beyond the formal lift-off 20mm.

For the case of successful trials of each of the lift-offs, we also calculated the normalized differences between the two largest extrema in likelihood functions (for mode number 3) in percentage as  $Q = |\xi_1 - \xi_2| / |\xi_1| \times 100\%$ , where  $\xi_1, \xi_2$  are respectively the likelihood values of the 1st and the 2nd maxima and  $|\cdot|$  represents the absolute value. Table 2 lists the minimum, the mean and the standard deviation of the normalized differences obtained from the successful trials for each of the lift-offs. We observe that with the increase of the lift-off, both the minimum as well as the mean of the normalized difference between the two extrema increases (up to the formal lift-off 20mm). This means that the maximum of the likelihood function becomes easily distinguishable. The fact enable us to achieve a reliable measurement in the diameter.

We also observe that the standard deviation of the normalized differences for the 20mm formal lift-off is large compared to those of other lift-offs. Such a result was obtained due to the fact that for some of the trials with the 20mm lift-off, the differences between the two extrema were found comparatively large, although the details are omitted here.

For reference, **Fig.11** shows the observation sequence for 0mm formal lift-off selected from one of the successful trials, while **Fig.12** shows another example of observation sequence for 20mm formal lift-off. After analyzing both of them by our signal processing method, we get the likelihood functions as shown in **Fig.13** and **Fig.14**. Although the maximum of the likelihood function lies within the allowable range of rib's pitch in the trial with the

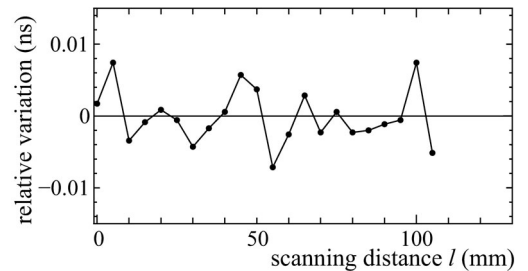


Fig. 11: Observation sequence for a successful trial for the formal lift-off 0mm

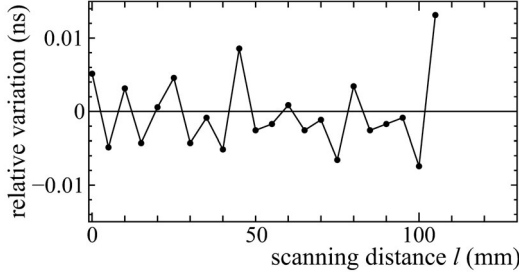


Fig. 12: Observation sequence for the formal lift-off 20mm

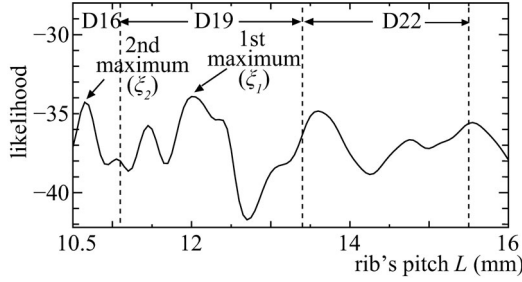


Fig. 13: Likelihood function for the formal lift-off 0mm

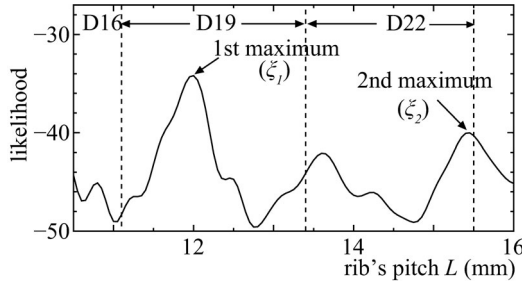


Fig. 14: Likelihood function for the formal lift-off 20mm

formal lift-off 0mm, the normalized difference between the two largest extrema is only 1.07%. However, for the 20mm formal lift-off, the normalized difference is as large as 17.02%. Therefore, the maximum of the likelihood function is more reliable to be accurately picked up as we increase the lift-off.

## 5. Conclusion

For the nondestructive inspection of the diameter of the deformed reinforcing bars in concrete, an EMW radar was proposed to use for scanning the bar while being lifted off the concrete surface. The experiments showed that with the increase of the lift-off a smaller angle of incidence of the EMW to the bar could be achieved, which in turn ensured the obtaining of a much more accurate propagation time of the EMW from the point (on the bar) just below the scanning point.

By applying our previous signal processing method, which applied a Kalman filter and maximum likelihood to a dynamic model of the propagation time variation along

the length of the bar, the success rate in the right identification of the rib's pitch (and consequently the diameter of the bar) was found to increase significantly. The proposed method was found to be much more reliable in measuring the diameter of the bar compared to our previous one.

## References

- 1) A.M. Neville, "Properties of Concrete," *Prentice Hall*, (1995)
- 2) H. Begum, M. Okamoto and S. Tanaka "Measurement of the Diameter of Deformed Reinforcing Bar in Reinforced Concrete Structure Using an Electromagnetic Wave Radar," *Proc. of the 39th ISCIE International Symposium on Stochastic Systems Theory and Its Applications*, 26/31 (2007)
- 3) S. Tanaka and M. Yamada, "Non-Destructive Inspection of Concrete using an Electromagnetic Wave (Radar) Based on a Signal Propagation Model," *Transaction of SICE*, **39**, 5, 432/440 (2003)
- 4) S. Tanaka, "An Accurate and Real Time Non-Destructive Inspection method of Tunnel Using an Electromagnetic Wave Radar," (in Japanese) *Journal of SICE*, **44**, 3, 173/179 (2005)
- 5) S. Tanaka, "Measurement Systems Engineering," *Asakura Pub. Co.*, (1994)
- 6) K. Hongo, "Fundamentals of Electromagnetic Wave Engineering," *Jikkyo Pub. Co.*, (1985)

## Appendix A.

The error function  $e(t)$  between the actual received signal  $r(t)$  and the modeled received signal  $\tilde{r}(t)$  is written as

$$\begin{aligned} e(t) &= r(t) - \tilde{r}(t) \\ &= r(t) - p_1 r_s(t - T_1) - p_2 r_o(t - T_2) \end{aligned} \quad (\text{A.1})$$

For any given values of  $T_1$  and  $T_2$ , the optimal values of  $p_1$  and  $p_2$  are obtained by minimizing the square of the error function ( $e^2(t)$ ) with respect to  $p_1$  and  $p_2$  respectively. The square of error function can be written in vector form as

$$\begin{aligned} \mathbf{e}^T \mathbf{e} &= (\mathbf{r} - p_1 \mathbf{r}_s - p_2 \mathbf{r}_o)^T (\mathbf{r} - p_1 \mathbf{r}_s - p_2 \mathbf{r}_o) \\ &= \mathbf{r}^T \mathbf{r} - 2p_1 \mathbf{r}_s^T \mathbf{r} - 2p_2 \mathbf{r}_o^T \mathbf{r} + p_1^2 \mathbf{r}_s^T \mathbf{r}_s \\ &\quad + p_2^2 \mathbf{r}_o^T \mathbf{r}_o + 2p_1 p_2 \mathbf{r}_o^T \mathbf{r}_s \end{aligned} \quad (\text{A.2})$$

Where,  $\mathbf{e}$ ,  $\mathbf{r}$ ,  $\mathbf{r}_s$  and  $\mathbf{r}_o$  are the vectors corresponding to the functions  $e(t)$ ,  $r(t)$ ,  $r_s(t)$  and  $r_o(t)$ , respectively. Now differentiating Eq.(A.2) with respect to  $p_1$  and  $p_2$  respectively and equating them to zero, we get

$$\begin{aligned} p_1 (\mathbf{r}_s^T \mathbf{r}_s) + p_2 (\mathbf{r}_o^T \mathbf{r}_s) &= \mathbf{r}_s^T \mathbf{r} \\ p_1 (\mathbf{r}_o^T \mathbf{r}_s) + p_2 (\mathbf{r}_o^T \mathbf{r}_o) &= \mathbf{r}_o^T \mathbf{r} \end{aligned} \quad (\text{A.3})$$

Finally, we get  $p_1^*$  and  $p_2^*$  as

$$\begin{bmatrix} p_1^* \\ p_2^* \end{bmatrix} = \begin{bmatrix} \mathbf{r}_s^T \mathbf{r}_s & \mathbf{r}_o^T \mathbf{r}_s \\ \mathbf{r}_o^T \mathbf{r}_s & \mathbf{r}_o^T \mathbf{r}_o \end{bmatrix}^{-1} \begin{bmatrix} \mathbf{r}_s^T \mathbf{r} \\ \mathbf{r}_o^T \mathbf{r} \end{bmatrix} \quad (\text{A. 4})$$

=====

**Halima BEGUM** (Student Member)



She received her BSc. in Electrical and Electronic Engineering from Bangladesh University of Engineering & Technology, Bangladesh in 2002 and received M.Engg. in Electrical and Electronic Engineering in 2007 from Yamaguchi University, Japan, and is currently enrolled in the doctorate course at the same University. Her current research interests include non-destructive inspection using electromagnetic wave radar, advanced signal processing and system modeling.

**Masayuki OKAMOTO**



He received the B.S. and the M.S. degrees both in electronic engineering from Yamaguchi University in 1994 and 1996 respectively. He then received Ph.D. degree in system engineering from the same University in 1999. Since 1999, he has been a Research Associate of Electrical & Electronic Engineering, Faculty of Engineering, Yamaguchi University. His current research interests lie in the intelligent sensing and the anomaly diagnosis. He received the Research and Technology Promotion Award from the Instrument Department of SICE (2002).

**Shogo TANAKA** (Member)



He received the B.S. degree in electronic engineering from Kyushu University in 1971, and the M.S. and Ph.D. degrees both in electrical engineering from the University in 1973 and 1979, respectively. From 1976 to 1979, he was with the Department of Electrical Engineering of the University as a Research Associate, and from 1979 to 1990, an Associate Professor of Electronic Engineering, Faculty of Engineering, Yamaguchi University. Since 1991, he has been a Professor of Electrical & Electronic Engineering of the University. His current research interests lie in the intelligent sensing and the anomaly diagnosis. He is a member of the Society of Instrument and Control Engineers (SICE), the Institute of Electrical Engineers of Japan and the Institute of Systems, Control and Information Engineers. He received the Chugoku Cultural Award (2003), the Award of the Japanese Ministry of Education and Science (2004) and SICE Awards (2005 and 2006). He is a fellow of SICE.

=====